A Simple Method to Measure the Local Geomagnetic Field Accurately in a First-Year Physics Laboratory

Cite as: Phys. Teach. **59**, 44 (2021); https://doi.org/10.1119/10.0003017
Published Online: 29 December 2020

Si Wang, Shiqi Huang, Chenchen Liu, et al.

A Simple Method to Measure the Local Geomagnetic Field Accurately in a First-Year Physics Laboratory

Si Wang, Shiqi Huang, Chenchen Liu, Ziqian Tang, Qingfan Shi, Beijing Institute of Technology, Beijing, China
Jurgen Schulte, University of Technology Sydney, Australia

The directional feature of Earth's geomagnetic field has been contributing to the technological development and prosperity of humankind since the invention of the magnetic compass navigation centuries ago. Today, for instance, magnetoresistance sensors are commonly used in nanosatellites and unmanned aerial vehicles for high accuracy geomagnetic field-based navigation and mineral survey exploration.[1-4]

In a first-year undergraduate physics laboratory, the measurement of the local geomagnetic field often serves to illustrate the vector and field nature of an original physics phenomenon, albeit often carried out in a more qualitative way due to the limited accuracy of available instrumentation. In this paper, we describe a simple and yet highly accurate method to determine the local geomagnetic field and its components. It provides an excellent opportunity for students to apply some basic calculus while also acquiring some data processing skills and glimpses of real scientific working.

A common method to investigate the magnetic field direction and its magnitude is to place a compass needle in the center of a solenoid (e.g., Helmholtz coil) that is oriented such that it generates an east-west oriented magnetic field.[6-9] The tangent value of the deflection angle of the compass needle relative to the direction of north-south then represents the ratio of the known solenoid field to the horizontal component of the local geomagnetic field. The horizontal component of the local magnetic field can thus be calculated. The vertical field component can be obtained by using a vertically aligned compass (dip needle). This method is quite intuitive as it can be easily visualized and hence is often illustrated in textbooks in this way. The accuracy of the geomagnetic field deflection angle reading though is limited by the set of scales on the compass with a typically error margin of about 10%.[10] A common, somewhat more sophisticated approach is to measure the oscillation of a cylindrical magnet polarized along its major axis as it reacts to the torque caused by the local geomagnetic field. This particular method neglects the vertical component of the field, resulting in a similar 10% uncertainty for the magnitude and direction of the local geomagnetic field.[10]

In this paper, we present a novel experimental approach to determine the local geomagnetic field based on equipment readily available in a first-year undergraduate physics program. The accuracy of the geomagnetic field measurement can be improved by using a cylindrical permanent magnet (CPM) that is placed at the center of a Helmholtz coil and measuring its periodical oscillation within the vertical plane containing the coil's axis (Fig. 1).

A simple theoretical model of the CPM's oscillation can be developed from first principles, and a numerical fit to measured oscillation periods then reveals accurate values for the local geomagnetic field and its components.

Some borrowing from calculus

For deriving the theoretical model of the CPM's oscillation in the Helmholtz field, we assume that the magnetic field $\boldsymbol{B}$ (the vector sum of the geomagnetic field $\boldsymbol{B}_e$ and magnetic field of the Helmholtz coil $\boldsymbol{B}_h$) is uniform within the dimension of the CPM, which is a reasonable assumption considering the high magnetic flux uniformity at the center of the coil and the dimensions of Earth and that of the CPM.

We lay out our coordinate system for the vector properties such that the Helmholtz field $\boldsymbol{B}_h$ is in the y-direction, the horizontal component of the geomagnetic field $\boldsymbol{B}_{e\text{-}hor}$ in the opposite y-direction, and the vertical component of geomagnetic field $\boldsymbol{B}_{e\text{-}ver}$ in the z-direction, so that $\boldsymbol{B}$ is in the yz-plane as shown in Fig. 1.

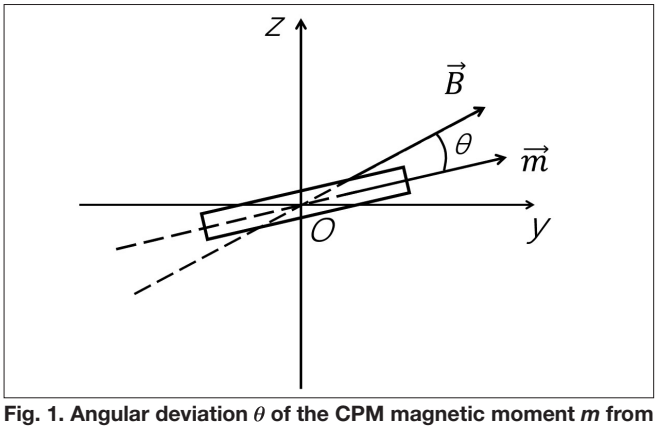

Fig. 1. Angular deviation θ of the CPM magnetic moment $\boldsymbol{m}$ from the static magnetic field $\boldsymbol{B}$ in the yz-plane.

When the CPM is at rest, its magnetic moment $\boldsymbol{m}$ aligns with the direction of $\boldsymbol{B}$. An oscillation about its center of mass in the yz-plane causes the magnetic moment $\boldsymbol{m}$ to deviate in its direction relative to $\boldsymbol{B}$ by an angle θ (Fig. 1).

The torque that the CPM is experiencing during its oscillatory motion is given by $\boldsymbol{\tau} = \boldsymbol{m} \times \boldsymbol{B}$.[11] For small oscillations ($\theta < 10^o$) in the yz-plane, we may approximate the torque by

$$|\boldsymbol{\tau}| = |\boldsymbol{m}| \cdot |\boldsymbol{B}| \cdot \sin\theta \approx |\boldsymbol{m}| \cdot |\boldsymbol{B}| \cdot \theta \,. \tag{1}$$

On the other hand, from the mechanics for rotating bodies we know that the torque is related to the angular acceleration $\ddot{\theta}$ by

$$|\boldsymbol{\tau}| = I(\ddot{\theta}), \tag{2}$$

with I the moment of inertia of a solid cylinder,[11]

$$I = \frac{1}{4} m_0 R^2 + \frac{1}{12} m_0 l^2, \tag{3}$$

and m_0 the CPM mass, R its radius, and l its length. With Eqs. (1) and (2) we are now in a position to derive the cylinder's equation of motion,

 DOI: 10.1119/10.0003017

$$I\ddot{\theta} - |\boldsymbol{m}| \cdot |\boldsymbol{B}| \cdot \theta = 0, \quad (4)$$

which is the familiar simple harmonic motion with angular frequency $\omega = \sqrt{|\boldsymbol{m}| \cdot |\boldsymbol{B}| / I} = 2\pi / T$, and T the period of oscillation. The magnetic field $\boldsymbol{B}$ may be written in terms of its components,

$$\boldsymbol{B} = \boldsymbol{B}_{\mathrm{e}} + \boldsymbol{B}_{\mathrm{h}} = (|\boldsymbol{B}_{\mathrm{h}}| - |\boldsymbol{B}_{\text{e-hor}}|)\,\boldsymbol{j} + |\boldsymbol{B}_{\text{e-ver}}|\,\boldsymbol{k}\ ,$$

with $\boldsymbol{j}$ and $\boldsymbol{k}$ the unit vectors in y- and z-direction, respectively. The magnitude of $\boldsymbol{B}$ is then

$$|\boldsymbol{B}| = \sqrt{(|\boldsymbol{B}_{\mathrm{h}}| - |\boldsymbol{B}_{\text{e-hor}}|)^2 + |\boldsymbol{B}_{\text{e-ver}}|^2} = \sqrt{(KI_0 - |\boldsymbol{B}_{\text{e-hor}}|)^2 + |\boldsymbol{B}_{\text{e-ver}}|^2}, \quad (5)$$

where I_0 is the excitation current in the Helmholtz coil and K a scalar parameter specifying the Helmholtz coil's sensitivity, i.e., the ratio of the Helmholtz magnetic field to its excitation current. With Eq. (5) and the oscillation period T related to the magnetic field $|\boldsymbol{B}|$ through the angular frequency ω, we are now in the position to link the period T to the geomagnetic field vectors and the applied Helmholtz current I_0,

$$\frac{1}{T^4} = \frac{|\boldsymbol{m}|^2}{16\pi^4 I^2}\left(|\boldsymbol{B}_{\mathrm{e}}|^2 - 2KI_0|\boldsymbol{B}_{\text{e-hor}}| + K^2 I_0^2\right). \quad (6)$$

The relationship derived here has only two variables, the period T and the applied Helmholtz current I_0, which makes it an ideal base for an experimental investigation into the local geomagnetic field. We can measure the period of the CPM oscillation as function of the applied Helmholtz current I_0, graph the resultant measurements in a T^{-4} vs. I_0 plot, and then determine the constant coefficients $\boldsymbol{B}_{\mathrm{e}}$ and $\boldsymbol{B}_{\text{e-hor}}$ from a best fit to the resulting T^{-4} period function.

Assembling and conducting the experiment

The essential pieces of this experiment are the Helmholtz coil, a power source, a CPM, and a common consumer camera for recording the CPM oscillation (Figs. 2 and 3). Ferromagnetic objects and electronic devices should be kept away from the experimental setup. A compass is used to line up the Helmholtz coil with Earth's magnetic north-south direction. The dimensions of the CPM used in our experiment were measured with a caliper; $l = 24.000 \pm 0.006$ mm and its cross-section diameter $d = 6.000 \pm 0.001$ mm. Its mass was measured on a scale, $m_0 = 4.800 \pm 0.056$ g. This allows us to calculate the CPM's inertia from Eq. (3), $I = 2.412\times10^2$ g·mm^2. The Helmholtz coil sensitivity parameter, $K = 4.08\times10^{-3}$ T/A, is provided with the manufacturer's specifications.

The CPM is suspended at the center of the Helmholtz coil by a fine horizontal thread (we used thin cotton thread) (Figs. 3 and 4). An initial, small change in the Helmholtz current I_0 triggers a noticeable oscillation of the CPM about the horizontal thread axis. Equation (6) provided us with the base for our experimental investigation, i.e., to measure the CPM's oscillation period for a range of Helmholtz trigger currents I_0 (1 mA – 14 mA).

For an accurate measurement of the oscillation period,

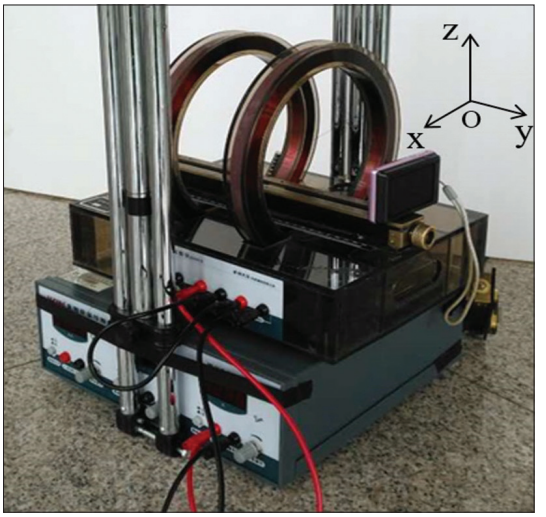

Fig. 2. Experimental setup with Helmholtz coil, camera, and power supply.

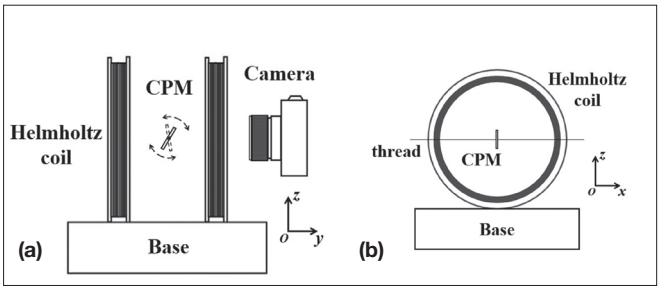

Fig. 3. Schematics of the experimental setup. (a) Front view (*zy*). (b) Side view (*zx*).

we used a common low-cost consumer camera (SONY DSC-TX5, 60 fps) to video record the CPM's oscillation. The camera is placed such that it faces the center of the Helmholtz coil (Figs. 2 and 3). The oscillation of the CPM is recorded once its initial amplitude has receded such that the oscillation angle with respect to the vertical is within the range of our theoretical small-angle approximation (<10°).

Figure 4(a) shows a video frame where the CPM is just about to swing through its half-period point. Figure 4(b) shows a frame where the end of a completed cycle has been reached, hence providing a simple way to measure oscillation periods.

For each Helmholtz excitation current, we determined the average oscillation period T from averaging over 50 oscillations. In this process, we neglected all non-conservative forces, which we assumed to be negligible.

The compactness of the experimental setup (Fig. 2) makes

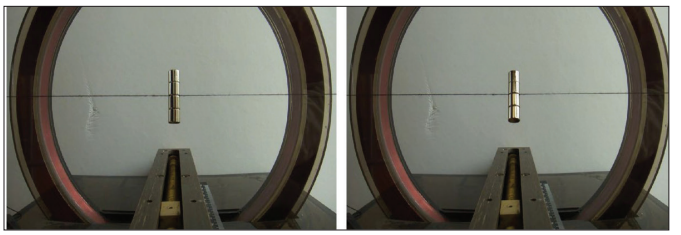

Fig. 4. Camera video frames of oscillating CPM. Half period (left) and period completed (right).

it easy for it to be used in extended student projects and at different locations. Here, we took measurements at three different locations: a dedicated undergraduate physics laboratory (L), a teaching building (T) about 1 km away from the laboratory, and a sports field (F) about 0.7 km away from the laboratory. This allows us to observe small variations in the local geomagnetic field at different locations.

Pulling the strings together

Once all measurements have been recorded, we can set out to finally determine the local geomagnetic field strength and its component by fitting the coefficients in the quadratic function in Eq. (6) to the quadratic function of measured oscillation periods (Fig. 5).

The best fits for our three locations are (where the currents are measured in mA and the period is measured in seconds):

$$\begin{aligned} \text{F:}\quad & \frac{1}{T^4} = 0.0588\, I_0^2 - 0.851\, I_0 + 11.20, \\ \text{T:}\quad & \frac{1}{T^4} = 0.0559\, I_0^2 - 0.809\, I_0 + 11.20, \\ \text{L:}\quad & \frac{1}{T^4} = 0.0537\, I_0^2 - 0.780\, I_0 + 11.20. \end{aligned} \tag{7}$$

The fit coefficients can now be related to the respective magnetic moments and fields in Eq. (6):

$$\frac{|\boldsymbol{m}|^2}{16\pi^4 I^2} K^2 = \begin{cases} 0.0588 \pm 0.0041\ \mathrm{s^{-4}mA^{-2}} \\ 0.0559 \pm 0.0027\ \mathrm{s^{-4}mA^{-2}} \\ 0.0537 \pm 0.0033\ \mathrm{s^{-4}mA^{-2}} \end{cases} \tag{8}$$

$$-\frac{2K|\boldsymbol{m}|^2}{16\pi^4 I^2}|\boldsymbol{B}_{\text{e-hor}}| = \begin{cases} -0.851 \pm 0.063\ \mathrm{s^{-4}mA^{-1}} \\ -0.809 \pm 0.041\ \mathrm{s^{-4}mA^{-1}} \\ -0.780 \pm 0.050\ \mathrm{s^{-4}mA^{-1}} \end{cases} \tag{9}$$

$$\frac{|\boldsymbol{m}|^2}{16\pi^4 I^2}|\boldsymbol{B}_{\text{e}}|^2 = \begin{cases} 11.20 \pm 0.21\ \mathrm{s^{-4}} \\ 11.08 \pm 0.14\ \mathrm{s^{-4}} \\ 11.00 \pm 0.17\ \mathrm{s^{-4}} \end{cases} \tag{10}$$

The first, second, and third rows on the right-hand side of Eqs. (8)-(10) correspond to the measurements in the sports field, teaching building, and the laboratory, respectively. It is worthwhile to mention that this method also measures the magnetic moment $|\boldsymbol{m}|$, which can be determined from the I_0^2 coefficient of the fit in Eq. (7).

With the CPM's moment of inertia I calculated from Eq. (3) and the magnetic moment $|\boldsymbol{m}|$ from Eq. (8), it is now a simple step to calculate the magnitudes of Earth's magnetic field $|\boldsymbol{B}_{\text{e}}|$, its horizontal $|\boldsymbol{B}_{\text{e-ver}}|$ and vertical $|\boldsymbol{B}_{\text{e-hor}}|$ components, and respective geomagnetic field inclinations α. Table I shows the magnitudes of the local geomagnetic field and its components derived from this simple experiment with the support of some basic calculus applied to our theoretical model. We also found small variations in field magnitudes and inclinations even for locations that were only short distances apart.

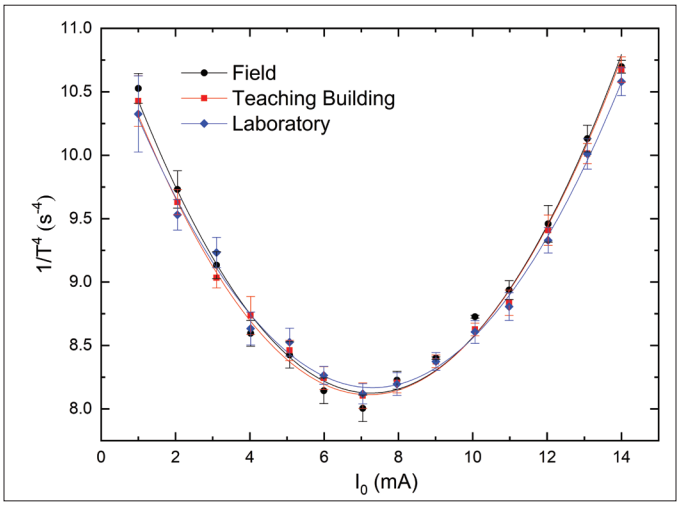

Fig. 5. Measured left-hand side of Eq. (9), i.e., T^{-4} (fitted to measured experimental values for various Helmholtz excitation currents I_0).

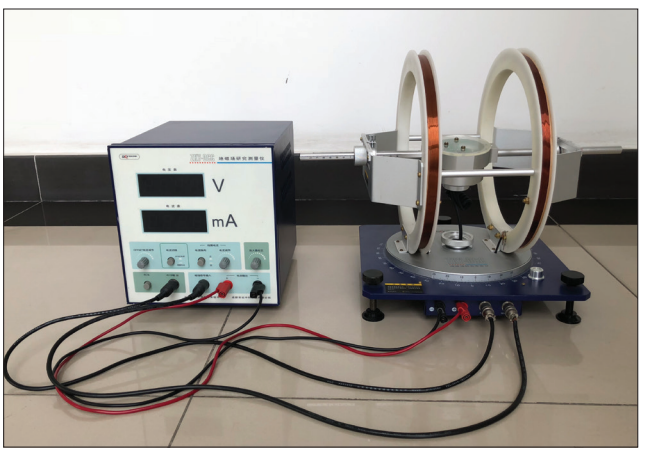

Fig. 6. ZKY-DCC Geomagnetic Field Instrument.

At this stage, we have completed three typical steps in a scientific investigation, finding an appropriate theoretical framework that applies to what we wish to measure, developing an experiment and experimental procedure for the measurement, and establishing a protocol for how we wish to evaluate our measurements. How do we know that our measurements of the local geomagnetic field are accurate?

We were fortunate that one of our more advanced student laboratories at BIT had a commercial high-precision geomagnetic magnetic field-measuring instrument (ZKY-DCC, Beijing Zhuozhang Electronic Science & Technology Co. Ltd.; Fig. 6) that we could use to compare our results with. Our results for the magnitude of the local geomagnetic field deviate by less than 2.5% from the measurements taken with the professional instrument, and respective geomagnetic inclinations α deviate by less than 1% (Table I). Our measured magnetic fields are all slightly larger than the ones measured with the commercial instrument. For a simple Helmholtz coil as used here, the sensitivity parameter K is often derived from an average coil radius rather than a precision field measurement. This may result in a larger than actual K value, which in turn causes a scaling of field values.

Table I. Magnitudes of local magnetic fields and respective inclinations from measurements in the field (F), teaching building (T), and laboratory class (L) compared to measurements with commercial purpose built ZKY-DCC instrument (ZKY subscripts). Magnetic fields in units of μT, angles in angle degrees.

	$\lvert B_{\text{e-hor}}\rvert$	$\lvert B_{\text{e}}\rvert$	$\lvert B_{\text{e}}\rvert_{\text{ZKY}}$	α	α_{ZKY}
F	29.50±0.04	56.30±0.03	55.12±0.08	58.399±0.012	58.439±0.020
T	29.56±0.17	57.47±0.10	56.19±0.14	59.038±0.022	59.144±0.020
L	29.64±0.24	58.42±0.35	57.11±0.20	59.507±0.015	59.558±0.025

Learning experience

We developed a novel approach to embed basic elements of calculus in the experimental measurement of the local geomagnetic field, which is based on commonly available first-year physics laboratory equipment. The experimental setup itself is easily assembled with a cylindrical permanent magnet suspended at the center of a Helmholtz coil and its oscillation recorded with a common consumer camera or mobile phone. The small number of components allows the local geomagnetic field measurement to easily be carried out at different locations, including outdoor field locations.

The method presented here includes a theoretical model that combines multiple physics concepts such as rotational kinematics and inertia, classical dynamics, and electromagnetics, which together with the experimental measurement allow us to accurately determine all components of the local geomagnetic field.

The presented approach engages students in an authentic scientific practice of physical modeling that is nontrivial, goes beyond textbook models and knowledge, and yet is entirely based on first-year fundamental physics. The experiment itself is simple to conduct, requiring only very basic experimental skills such as setting an electric current and observing the period of oscillation of the CPM. This simplicity enables students to conduct the experiment independently with little supervision, even outside the classroom environment. The setting up of the experiments takes about 10 minutes, the measurements take about 20 minutes per location, and the post-experiment video analysis takes another 20 minutes per location set.

The evaluation of the experimental data requires some mathematical modeling, i.e., fitting of a nonlinear function and respective error analysis. This can be done with a common data analysis software, or as part of a larger student project or teaching module across a physics and mathematics course.

The presented student experiment shows how the application of a sophisticated physical model based on a simple experimental setup can produce very accurate outcomes for the measurement of a nontrivial phenomenon, here Earth's local geomagnetic field components and its inclination. With the low-level experimental approach taken here, we found the measurements highly reproducible and of high accuracy even when compared to a sophisticated commercial magnetic field measuring instrument. The simplicity of the experimental approach applied to a nontrivial phenomenon offers an opportunity for lateral as well as project-based collaborative teaching and learning at junior undergraduate level.

References

1. Xiangyu Li, Jianping Hu, Weiping Chen, Liang Yin, and Xiaowei Liu, "A novel high-precision digital tunneling magnetic resistance-type sensor for the nanosatellites' space application," *Micromachines* **9** (121), 1–18 (2018), doi:10.3390/mi9030121.
2. Y. Guo and Y. Ouyang, "Exchange-biased anisotropic magnetoresistive field sensor," *IEEE Sens. J.* **17** (11), 309-3315 (2017).
3. J. Lenz and A. S. Edelstein, "Magnetic sensors and their applications," *IEEE Sens. J.* **6** (3), 631–649 (2006).
4. Z. Hui, L. Chuanjun, and L. Yukuan, "Research on ground calibration technology for geomagnetism sensors," *ICMME MATEC Web of Conferences* **153**, 07002 (2018), https://doi.org/10.1051/matecconf/201815307002.
5. A. Sameer and A. Hussein, "Measuring the Earth's magnetic field dip angle using a smartphone-aided setup: A simple experiment for introductory physics laboratories," *Eur. J. Phys.* **38**, 025201 (2017).
6. J. E. Williams, "Measuring Earth's local magnetic field using a Helmholtz coil," *Phys. Teach.* **52**, 236–238 (April 2014).
7. S. Ganci, "A simple measurement of the Earth's magnetic field," *Eur. J. Phys*. **25**, 475–477 (2004).
8. G. B. Stewart, "Measuring Earth's magnetic field simply," *Phys. Teach*. **38**, 113–114 (Feb. 2000).
9. R. A. Schill and K. Hoff, "Characterizing and calibrating a large Helmholtz coil at low ac magnetic field levels with peak magnitudes below the Earth's magnetic field," *Rev. Sci. Instrum*. **72**, 2769–2776 (2001).
10. A. Cartacci and S. Straulino, "Measuring the Earth's magnetic field in a laboratory," *Phys. Educ.* **43**, 412–416 (2008).
11. Edward M. Pureel, *Berkeley Physics Course* (McGraw-Hill Education, Asia, 2014).
12. A. Charles Kittel and C. Helmholz, *Mechanics* (McGraw-Hill Education, Asia, 2014).

Si Wang, Shiqi Huang, Chenchen Liu, Ziqian Tang, *undergraduate students, Beijing Institute of Technology;*
siwangbit@163.com

Qingfan Shi, *School of Physics, Beijing Institute of Technology;*
qfshi123@bit.edu.cn

Jurgen Schulte, *recipient of the Australian National Teaching & Learning Award; University of Technology Sydney, Australia;.*
jurgen.schulte@uts.edu.au